photoelectric emission depending on the previous treatment of the metal, but relative values for molybdenum and tungsten are not much affected by heat treatment. The emission from molybdenum is about 70% that from tungsten.

Experiments with an absorption screen of aluminium, 0·02 mm. thick, show that the photoelectric emission is produced mainly by the very soft components of the radiation.

The Flow Past Circular Cylinders at Low Speeds.

By A. Thom, D.Sc., Ph.D., Carnegie Teaching Fellow, University of Glasgow.

(Communicated by G. I. Taylor, F.R.S.—Received April 24, 1933.)

[Plates 10–13.]

Introduction.

This paper deals chiefly with calculations and experiments on the flow past circular cylinders, but the arithmetical methods of solution of the equations of steady viscous flow proposed and used in Section I, are applicable to other equations and may be of interest.

Section I.—*Arithmetical Methods of Solving the Equations of Viscous Steady Flow.*

The equations to be solved are

$$\left.\begin{aligned} \nu\,\nabla^2\zeta &= \frac{\partial\psi}{\partial x}\frac{\partial\zeta}{\partial y} - \frac{\partial\psi}{\partial y}\frac{\partial\zeta}{\partial x} \\ \nabla^2\psi &= 2\zeta \end{aligned}\right\}. \qquad (1)$$

The method of solution used* is one of repeated interpolation in a field of initially assumed values. As the formulæ of interpolation used involve the equations to be solved the values tend to settle to a solution provided certain precautions are taken. In practice the field is divided into squares and initially assumed values of ψ and ζ are written at each corner. In general the values at the centre of a square of side $2n$ are given by

$$\zeta_C = \zeta_M - \tfrac{1}{2}n^2\nabla^2\psi, \quad \psi_C = \psi_M - \tfrac{1}{2}n^2\nabla^2\psi, \qquad (2)$$

* Thom and Orr, 'Proc. Roy. Soc.,' A, vol. 131, p. 30 (1931); Thom, 'Aer. Res. Ctee.,' R. & M., No. 1194 (1929).

where

$$\psi_M = (A + B + C + D) \div 4$$
$$\zeta_M = (a + b + c + d) \div 4,$$

A, B, C and D are the corner values of ψ and a, b, c and d are the corresponding values of ζ.

These expressions, which are easily obtained by applications of Taylor's Theorem, are correct up to and including ∂^3 terms. In the particular case under consideration, namely, the solution of equations (1) above we obtain :—

$$\left.\begin{aligned} \zeta_C &= \zeta_M - \tfrac{1}{2}\frac{n^2}{\nu}\left(\frac{\partial\psi}{\partial x}\frac{\partial\zeta}{\partial y} - \frac{\partial\psi}{\partial y}\frac{\partial\zeta}{\partial x}\right) \\ \psi_C &= \psi_M - n^2\zeta_C \end{aligned}\right\}. \tag{3}$$

Writing approximate values for $\partial\psi/\partial x$, $\partial\zeta/\partial y$, etc., the final working form of these become :—

$$\left.\begin{aligned} \zeta_C &= \zeta_M - \frac{1}{16\nu}\{(a-c)(B-D) + (b-d)(C-A)\} \\ \psi_C &= \psi_M - n^2\zeta_C \end{aligned}\right\}. \tag{4}$$

Having used these to find the values at the centres of all squares they are used again to find new values at the original corners. The process is repeated over and over again till the values all over the field have settled. At solid boundaries the values of ζ on the surface are obtained from the approximate expression :—

$$\zeta = (\psi_G - \psi_S) \div m, \tag{5}$$

where ψ_S = value of ψ on the surface, and ψ_G = value of ψ at a point G distant m from the surface. This expression (or an equivalent) has to be used each time the squares are gone over.

If the squares used are too large the process may not be convergent, and even if convergent distorted results may be obtained.

As an example of the process consider the flow past a circular cylinder at Reynolds' Number $(Vd/\nu) = 10$. Part of the solution is shown in fig. 1. The particulars are : undisturbed velocity = 6·25, cylinder diameter = 10, coefficient of kinematic viscosity ν = 6·25. It will be seen that throughout the greater part of the field the ψ and ζ values are repeating to a reasonable accuracy, indicating that an approximate solution has been obtained. The streamlines thus obtained are shown in fig. 2. When the approximation is carried further there is an indication of negative values of ψ and ζ just behind the cylinder showing the presence of a small weak eddy. Further work on

this field has, however, not been carried out as a different method of procedure presented itself.

It will be realized that considerable difficulty arises at a curved boundary because it is impossible to arrange matters so that the boundary passes through

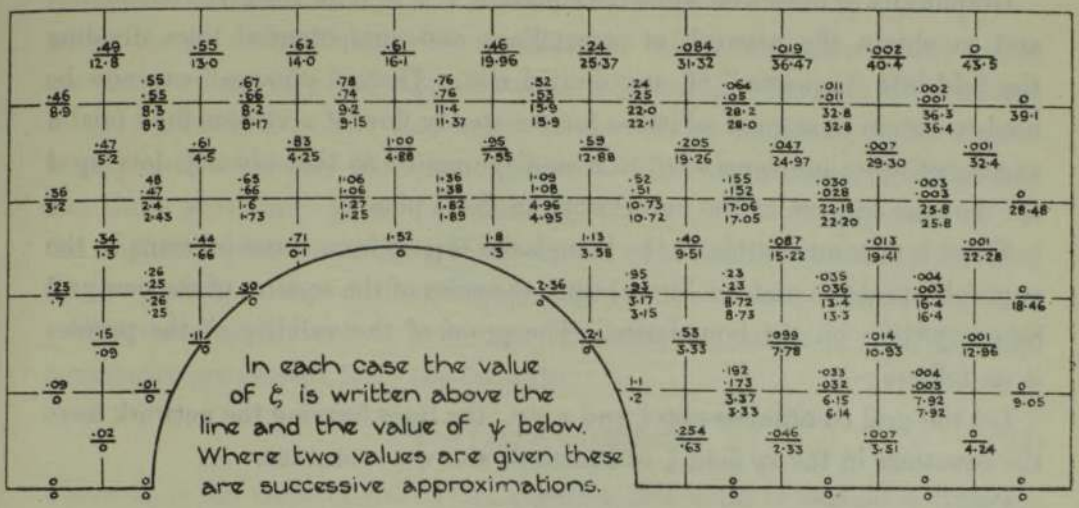

FIG. 1.

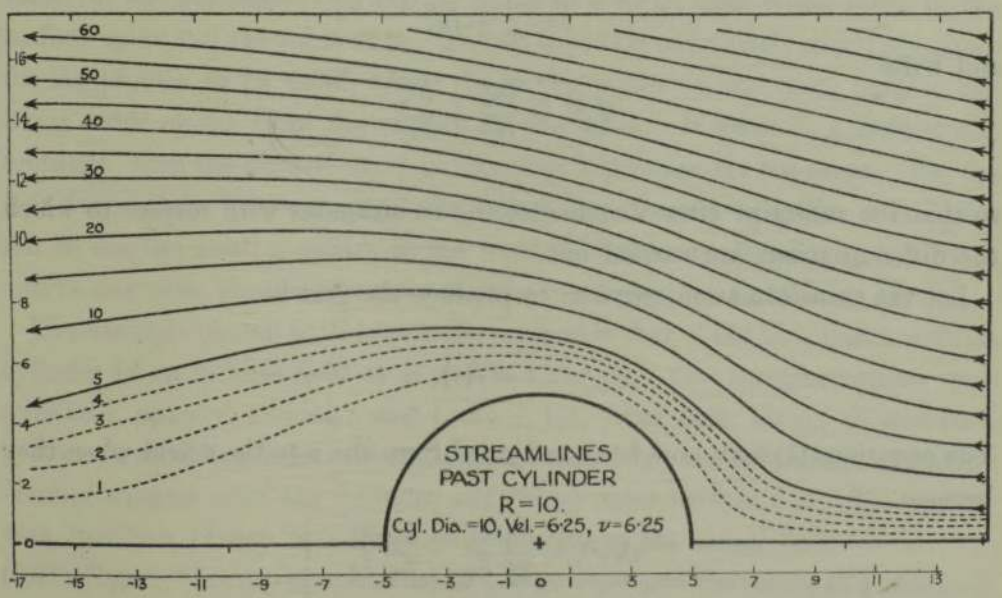

FIG. 2.

the corners of all the squares it cuts. Accordingly some method of interpolation has to be used to obtain the values of ψ and ζ for the successive approximations on the corners of those boundary squares whose outer corners

fail to fall exactly on the boundary. With fields of this type (and naturally they are in a majority) there is also more difficulty in calculating the ζ values on the solid boundaries.

These difficulties are both overcome by the following method.

Graphically or otherwise solve the equation $\nabla^2\psi = 0$ for the given boundaries and so obtain the network of streamlines and equipotential lines dividing the field into "squares" of any desired size. These "squares" can now be used to obtain numerical solutions for the steady flow of a viscous fluid (and a variety of other problems also) in a similar manner to that already developed for the true squares of the xy network in the z plane.

There is now no trouble at the boundaries (apart from those inherent in the particular problem under solution) since the sides of the squares of the new grid lie everywhere on the boundaries. The proof of the validity of the process is as follows :—

Let the grid co-ordinates be ξ and η, *i.e.*, the lines forming the network have the equations in the xy field $\xi =$ constant, and $\eta =$ constant.

Put

$$z = x + iy$$

$$t = \xi + i\eta,$$

and write

$$\nabla_t^2\zeta \equiv \frac{\partial^2\zeta}{\partial\xi^2} + \frac{\partial^2\zeta}{\partial\eta^2},$$

so that the subscript after ∇ indicates the co-ordinates with respect to which the differentiations are carried out.

Let the transformation required to produce the grid be

$$t = f(z).$$

The equations (1) may now be transformed from the z to the t field when they become

$$\left.\begin{aligned} \nu\nabla_t^2\zeta &= \frac{\partial\psi}{\partial\xi}\frac{\partial\zeta}{\partial\eta} - \frac{\partial\psi}{\partial\eta}\frac{\partial\zeta}{\partial\xi} \\ q^2\nabla_t^2\psi &= 2\zeta \end{aligned}\right\}. \qquad (6)$$

These equations only differ from those for the z field by the q^2 in the second member, and hence the method of treatment already described applies to their solution. q is the velocity of transformation.

The working formulæ are

$$\left.\begin{aligned}\zeta_C &= \zeta_M - \frac{1}{16\nu}\{(a-c)(B-D)+(b-d)(C-A)\}\\ \psi_C &= \psi_M - n^2\zeta_C/q^2\end{aligned}\right\}, \qquad (7)$$

where the subscript M indicates the mean of the corner values, small letters are corner values of ζ and capitals corner values of ψ. The side of the square in the t plane is $2n$. The true length of the side of the square in the z plane is $2n/q$ so that actually there is no difference whatever between these formulæ and those previously given. In working, however, it is inconvenient to use the original z plane with the grid drawn on. Instead the sheets are prepared for the t plane so that ordinary squared paper can be used (*e.g.*, see fig. 3).

When new corner values have been obtained, the values of ζ on the solid boundaries are revised from the formulæ

$$\zeta = (\psi_G - \psi_S)\, q^2/m^2, \qquad (8)$$

where ψ_G is the value of the stream function at a point G, distant m from the boundary in the t plane, that is at a distance m/q in the z plane, and ψ_S is the value on the boundary. In (8) the value of q to be used is the mean of the surface value and the value at G. To test that G is sufficiently near the surface for the process to be valid, apply (8) to two points on the same normal, one being twice as far from the surface as the other. If there is a serious discrepancy, then the distance even of the inner is presumably too large. For the first few rounds, however, until the values have begun to settle, it is better not to use too small a square as the work is thereby rendered very laborious, and in any case, the discrepancies may be due to the field not being settled.

The example chosen to illustrate the method is that of the flow past a circular cylinder in an infinite field at R = 20. For this, two transformations were available, namely, $t = \log z$ and $t = z + 1/z$. The first, giving as it does a system of radiating lines and concentric circles, has the advantage of having smaller squares near the cylinder and larger ones further out. The second was, however, chosen because of its similarity to the actual flow.

The " grid " having been plotted to a large scale and the values of q obtained the calculation of the viscous flow was commenced using the following values :—

d = cylinder diameter = 2

V = undisturbed velocity = 1

$\nu = 0{\cdot}1$

giving

$$R = Vd/\nu = 20.$$

To start the solution values of the vorticity ζ, and stream-function ψ were roughly estimated from the approximate solution for $R = 10$ already obtained. These having been written on the corners of squares in the t field, the work commenced. Formulæ (7) and (8) were applied until the field had settled.* In choosing the initial values no attempt was made to assume an eddy condition by writing negative values behind the cylinder. All the initially assumed values were positive. The negative values developed during the work, indicating a pair of symmetrical eddies in this region.

A portion of the work is shown in fig. 3. The sheet shown includes the eddy region. If a sample calculation is made it will be seen that no addition to the standard formulæ is required to deal with the eddy, in fact here the work is lightened as the second term in the formulæ (7) is so small in the eddy region as to be almost negligible, and $\nabla^4\psi = 0$ almost applies here. Fig. 3 also indicates how the size of square used varied, being generally larger the greater the distance from the cylinder. The criterion for the size of square is to try smaller squares and if serious differences are obtained, all the squares in the neighbourhood must be reduced in size.

It was found necessary to use very small squares in the region adjacent to the front generator—possibly because this is a singular point in the grid. The method of treating this region was substantially the same as that indicated elsewhere for the sharp intruding corner in the problem of the sudden expansion in a pipe.†

The whole process is long and no claim is made that the values obtained are perfect. The use of smaller squares everywhere would probably cause slight changes. It is, however, considered that the solution is better than that obtained previously for $R = 10$. The values of ψ and ζ obtained are shown plotted as contours in the t field in fig. 4. By means of the " grid " and some cross-plotting it is easy to obtain the actual streamlines. These are shown in fig. 5. The eddy is clearly shown in both figs. 4 and 5. It will be seen to correspond closely with the actual photographs of the eddy shown in Section 3. In size, it is nearest to the photograph at $R = 29$ (see fig. 12 (*d*), Plate 13).

* With regard to the number of repetitions required at a point, it is impossible to give a definite figure. It would depend on the boundaries, size of square, accuracy of the assumed solution, the accuracy of the required solution, and the position of the point in the field. Usually the number lies between 5 and 50.

† 'Aero. Res. Ctee.,' R. & M., No. 1475 (1932).

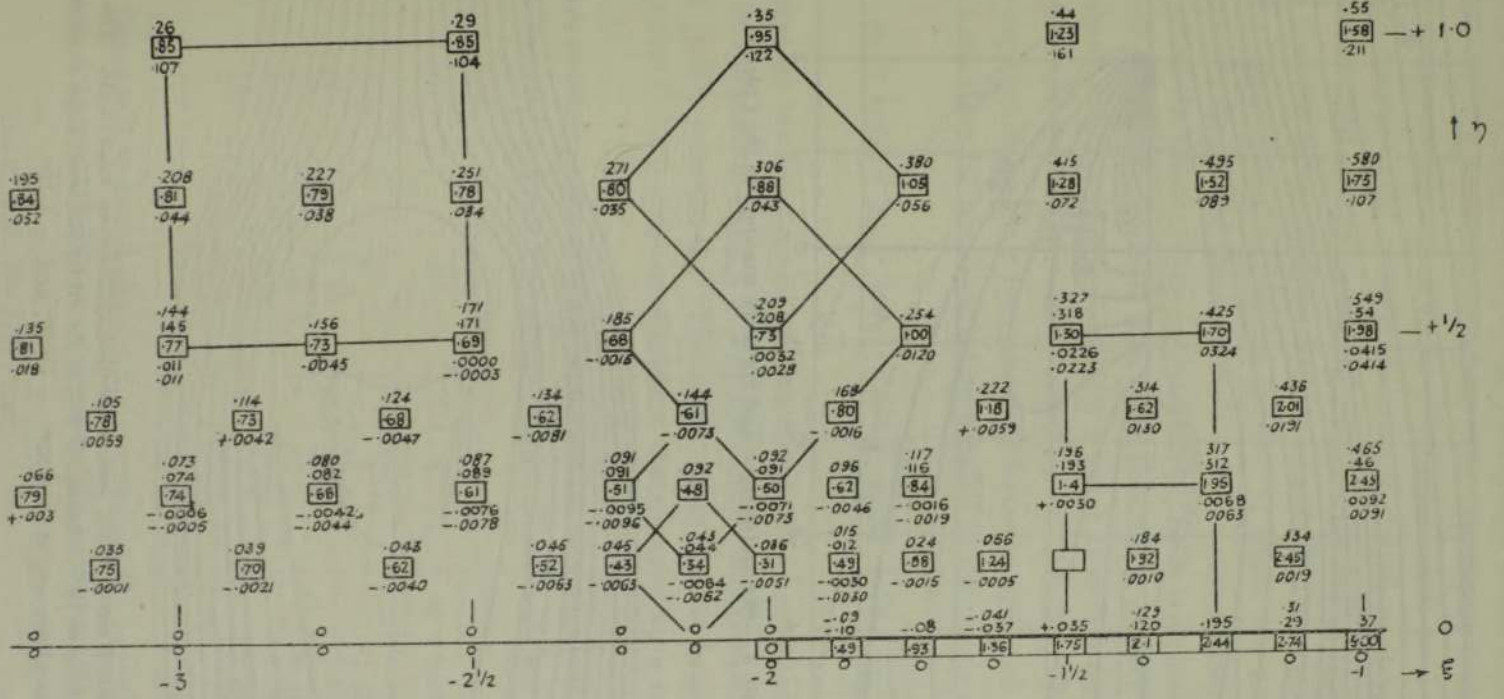

FIG. 3.—A portion of the working including the eddy region. Figures shown thus 0·082 were first taken from a previous sheet; from these the sloping figures were calculated. Values of q^2 are enclosed in rectangles. Values of ζ are written above the rectangle and values of ψ below.

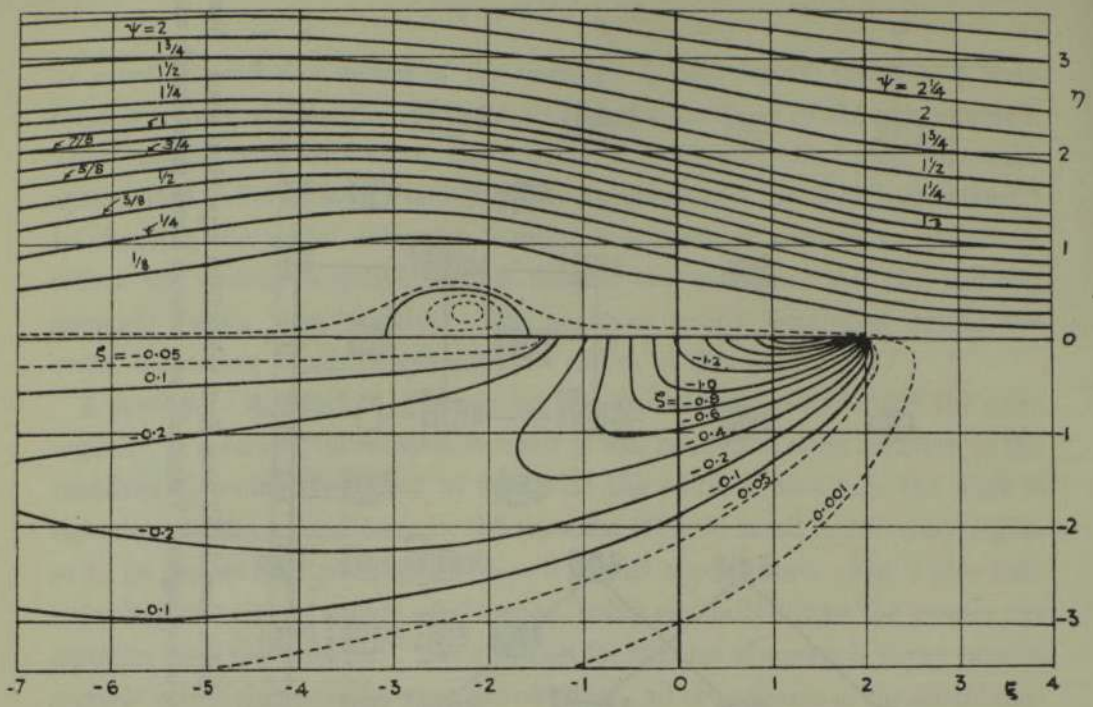

FIG. 4.—Streamfunction and vorticity contours in the t plane.

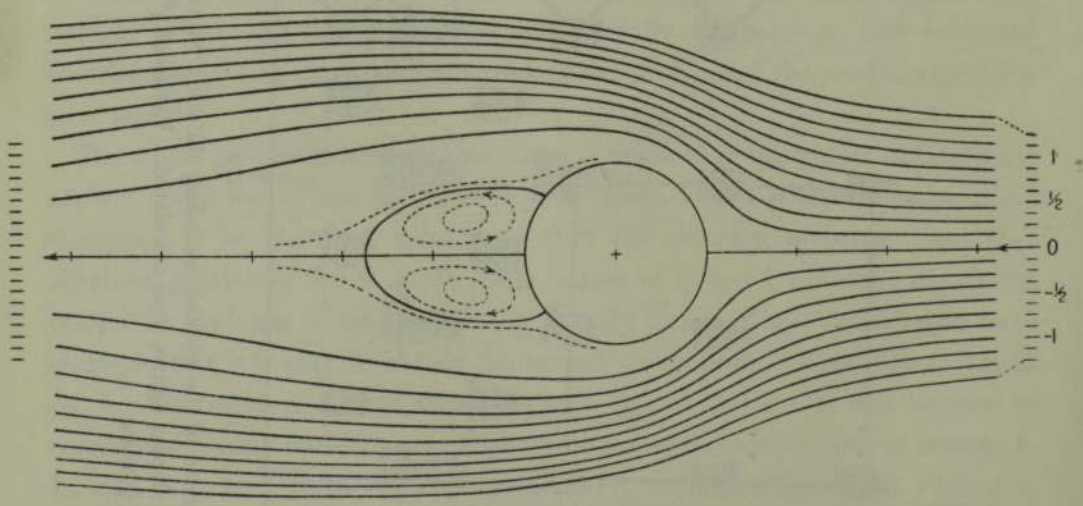

FIG. 5.—Calculated streamlines past a circular cylinder at $Vd/\nu = 20$. The spacing of the streamlines in the undisturbed flow is shown by the short lines at each end. The dotted streamlines are at $+ 1/256$, $- 1/256$, and $- 1/128$.

Fig. 5 can also be compared with the photograph obtained at R = 23 (see fig. 9, Plate 10). A further comparison with experiment is shown in fig. 13 where the maximum separation of the streamlines which were originally at a distance apart equal to the cylinder diameter is plotted on Reynolds' number. These were obtained from a number of photographs similar to fig. 9, Plate 10. It is seen that the value obtained from the theoretical streamlines is in good agreement. The distance behind the cylinder at which this maximum occurs is also shown in fig. 13 and the agreement is here again satisfactory.

To determine the pressure at any point A in the field it is necessary to integrate along a line from some point B where the pressure is already known to A.* In the present example B is conveniently a point at such a distance from the cylinder that the flow there is undisturbed by the cylinder. In deducing the necessary expressions for use in the t plane the factor q cancels out. For example Bernoulli's equation for use along a line parallel to the η axis is

$$p_A + \tfrac{1}{2}\rho q_A^2 = p_B + \tfrac{1}{2}\rho q_B^2 - 2\rho\nu \int_A^B \frac{\partial\zeta}{\partial\xi}\, d\eta + 2\rho \int_A^B \frac{\partial\psi}{\partial\eta}\, d\eta.$$

The pressure on the front generator was obtained by integrating along $\eta = 0$, and also by integrating along $\xi = 2$ in the t field. The results are 1·31 ($\frac{1}{2}\rho V^2$) and 1·35 ($\frac{1}{2}\rho V^2$) respectively. The mean value 1·33 is in good agreement with the value (1·335) obtained elsewhere theoretically by a totally different process.†

Pressures at other points on the cylinder surface were obtained by integrating along lines parallel to the η axis in the t field. The results are as follows :—

ξ.	ζ_0.	θ.	$(p - p_0)/\frac{1}{2}\rho V^2$.
2·0	0	0	+1·33
1¾	1·75	29·0	+0·67
1½	2·1	40·3	+0·12
1	2·0	60·0	−0·52
0	1·18	90·0	−1·16
−1½	0·03	139·7	−0·87
−2	0	180·0	−0·73

These values will be found plotted in fig. 6 among the experimental curves. The pressure drag is easily found. Expressed as a coefficient it is $K_D = 0{\cdot}624$.

* See R. & M., No. 1194 (1929).

† 'Aero Res. Ctee.,' R. & M., No. 1389, Table 5 (1931).

It has been shown elsewhere that the tangential force at a point is $2\mu\zeta_0$,* where ζ_0 is the value of the vorticity on the surface. The values of ζ_0 are given in the above table. Integrating the drag component of the tangential force and expressing the result as a coefficient gives $K_D = 0{\cdot}433$. Thus the

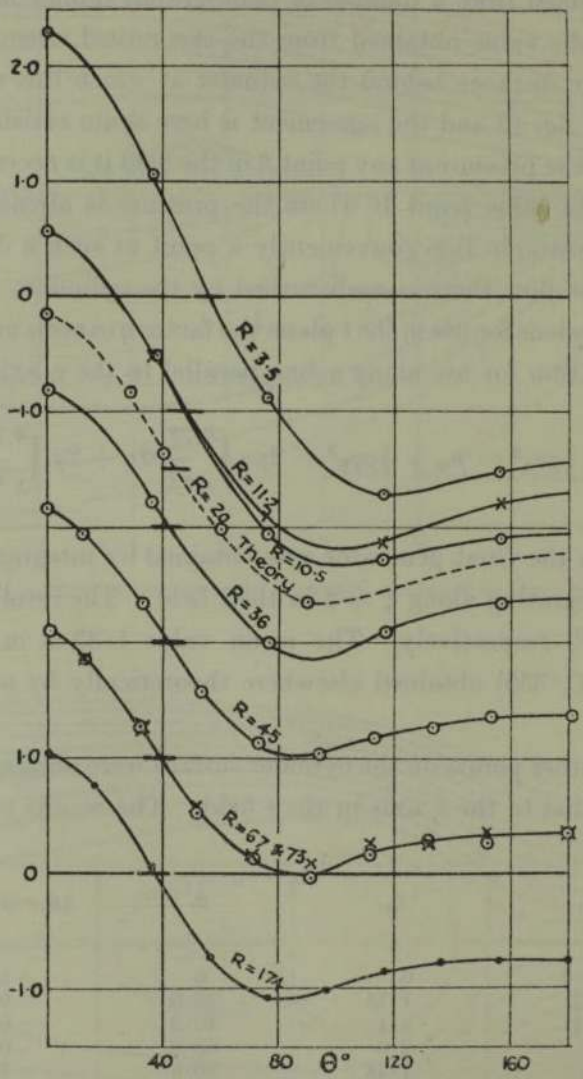

FIG. 6.—Pressure distribution round circular cylinders, experiments in oil and water. Ordinates are $(p - p_0) \div \frac{1}{2}\rho V^2$. The short thick black lines show zero (*i.e.*, static pressure for the curves which they cut).

total drag coefficient is $1{\cdot}057$ at $R = 20$, a result lying between the experimental values of Relf and those of Wieselberger. These results are shown on fig. 8 plotted along with experimentally determined values.

* *Loc. cit.*, R. & M., No. 1194; 'Aero. Res. Ctee.,' R. & M., No. 1389.

Section 2.—*Experimental Determination of the Pressure Distribution Round Circular Cylinders at Low Reynolds' Numbers in Oil and Water.*

The apparatus used was substantially that described in R. & M., No. 1389, and consists of a tank or channel having a working section 5 inches by 5 inches, and a form of Chattock gauge. At low speeds with small cylinders oil is more troublesome than water. This is partly on account of the greater coefficient of expansion of oil at the temperatures used. All leads have to be protected from temperature variation as pressure variations are produced by the slightest change in temperature such as that caused by a hand held near a part of the system. The reason is that the expanding oil is throttled by the very small hole or holes in the cylinder. To appreciate this it should be realized that the pressures to be measured are sometimes only a few thousandths of an inch of water. As the response of the gauge is very slow it takes a considerable time (up to an hour in some cases) to take a single reading of pressure.

The velocity was obtained from the measurements themselves by using the relation given in R. & M., No. 1389 between velocity and front generator pressure. Particulars of the oil used will also be found in that paper.

The static hole was on the channel wall opposite the cylinder, but even so a correction for wall effect is required. The exact amount of this connection is uncertain and the value used was, in the absence of better information, that given in the Appendix to R. & M., No. 1194. This uncertainty makes the measurements made with the smaller cylinders more reliable (other things being equal).

The final results are given in Table I which also contains an explanation giving the method of correction. The procedure of correcting the angles by $\frac{1}{2}h/d$ to allow for the size of the hole is fully justified at higher speeds but not yet at these low values of R (h = hole diameter). The results are plotted in fig. 6.

The values of the coefficient of pressure drag deduced from the values in Table I, are given in Table II, and will be found plotted in fig. 8 along with those from experiments in air (R. & M., No. 1194) and recent results by Linke* who having measured the total drag of cylinders under conditions identical to those obtaining when he measured the pressures, obtains reliable values for the part of the drag due to skin friction. His results bear out the expression given by the writer for the skin friction drag of a cylinder, namely, $K_D = 2 \div \sqrt{R}$†.

* 'Phys. Z.,' vol. 32, p. 900 (1931).

† 'Aero. Res. Ctee.,' R. & M., No. 1176 (1928).

Table I.

Oil. R = 3·5.

$t = 15{\cdot}0°$ $\nu = 0{\cdot}400$
$d = 0{\cdot}318$ $h = 0{\cdot}045$
$\epsilon = 0{\cdot}005$ V = 4·4

θ.	$\theta - \Delta\theta$.	p'.
0	0	2·3
40	36	1·05
80	76	−0·88
120	116	−1·72
160	156	−1·52

Oil. R = 10·5.

$t = 15{\cdot}0°$ $\nu = 0{\cdot}406$
$d = 0{\cdot}96$ $h = 0{\cdot}11$
$\epsilon = 0{\cdot}022$ V = 4·4

θ.	$\theta - \Delta\theta$.	p'.
0	0	1·56
40	37	0·49
80	77	−1·07
120	117	−1·29
160	157	−1·10

Oil. R = 11·2.

$t = 15{\cdot}7°$ $\nu = 0{\cdot}396$
$d = 0{\cdot}318$ $h = 0{\cdot}045$
$\epsilon = 0{\cdot}005$ V = 13·9

θ.	$\theta - \Delta\theta$.	p'.
0	0	1·54
40	36	0·48
80	76	−0·91
120	116	−1·13
160	156	−0·79

Oil. R = 36.

$t = 15°$ $\nu = 0{\cdot}410$
$d = 0{\cdot}96$ $h = 0{\cdot}11$
$\epsilon = 0{\cdot}022$ V = 14·5

θ.	$\theta - \Delta\theta$.	p'.
0	0	1·19
40	37	0·21
80	77	−1·00
120	117	−0·90
160	157	−0·65

Water. R = 45.

$t = 14°$ $\nu = 0{\cdot}0118$
$d = 0{\cdot}142$ $h = 0{\cdot}04$
$\epsilon = 0{\cdot}001$ V = 3·75

θ.	$\theta - \Delta\theta$.	p'.
0	0	1·16
20	12	0·93
40	32	0·35
60	52	−0·42
80	72	−0·87
100	92	−0·96
120	112	−0·81
140	132	−0·73
160	152	−0·61
180	180	−0·62

Water. R = 67.

$t = 14°$ $\nu = 0{\cdot}0118$
$d = 0{\cdot}142$ $h = 0{\cdot}04$
$\epsilon = 0{\cdot}001$ V = 5·6

θ.	$\theta - \Delta\theta$.	p'.
0	0	1·11
20	12	0·88
40	32	0·29
60	52	−0·48
80	72	−0·89
100	92	−1·04
120	112	−0·82
140	132	−0·70
160	152	−0·73
180	180	−0·64

Water. R = 73.

$t = 13{\cdot}6°$ $\nu = 0{\cdot}0119$
$d = 0{\cdot}142$ $h = 0{\cdot}04$
$\epsilon = 0{\cdot}001$ V = 6·1

θ.	$\theta - \Delta\theta$.	p'.
0	0	1·10
20	12	0·87
40	32	0·28
60	52	−0·43
80	72	−0·86
100	92	−0·92
120	112	−0·73
140	132	−0·71
160	152	−0·63
180	180	−0·64

Water. R = 174.

$t = 14{\cdot}4°$ $\nu = 0{\cdot}0117$
$d = 0{\cdot}318$ $h = 0{\cdot}045$
$\epsilon = 0{\cdot}005$ V = 6·4

θ.	$\theta - \Delta\theta$.	p'.
0	0	1·043
20	16	0·786
40	36	0·057
60	56	−0·713
80	76	−1·085
100	96	−1·002
120	116	−0·840
140	136	−0·769
160	156	−0·761
180	180	−0·739

$R = Vd/\nu$.
t = temperature °C.
ν = kinematic viscosity cm.²/sec.
d = cylinder diameter cm.
h = hole diameter, cm.
r = (channel width) ÷ d.
$\epsilon = 13 \div (30r + r^2)$.
V = fluid velocity, cm./sec.
$p' = p_1(1 - 2\epsilon) \div \frac{1}{2}\rho V^2$.
p_1 = observed pressure difference.

$$\Delta\theta = \frac{h}{2d}.$$

$$p' = \frac{p - p_0}{\frac{1}{2}\rho V^2}$$

Table II.

Cylinder diameter (cm.).	Fluid.	Fluid Velocity (cm./sec.).	Reynolds' number.	Coefficient of pressure drag.
0·318	Oil	4·4	3·5	1·325
0·96	,,	4·4	10·5	0·90
0·318	,,	13·9	11·2	0·71
0·96	,,	14·5	36·0	0·49
0·142	Water	3·75	45·0	0·46
0·142	,,	5·6	67·0	0·46
0·142	,,	6·1	73·0	0·45
0·318	,,	6·4	174·0	0·48

The present experiments deal, however, with a different range of Reynolds' numbers (R = 3·5 to R = 240). The determinations of drag by Relf and Wieselberger* from force measurements and the difference between the mean of these and the writers' determination of pressure drag, this difference being the skin friction drag, are also shown in fig. 8.

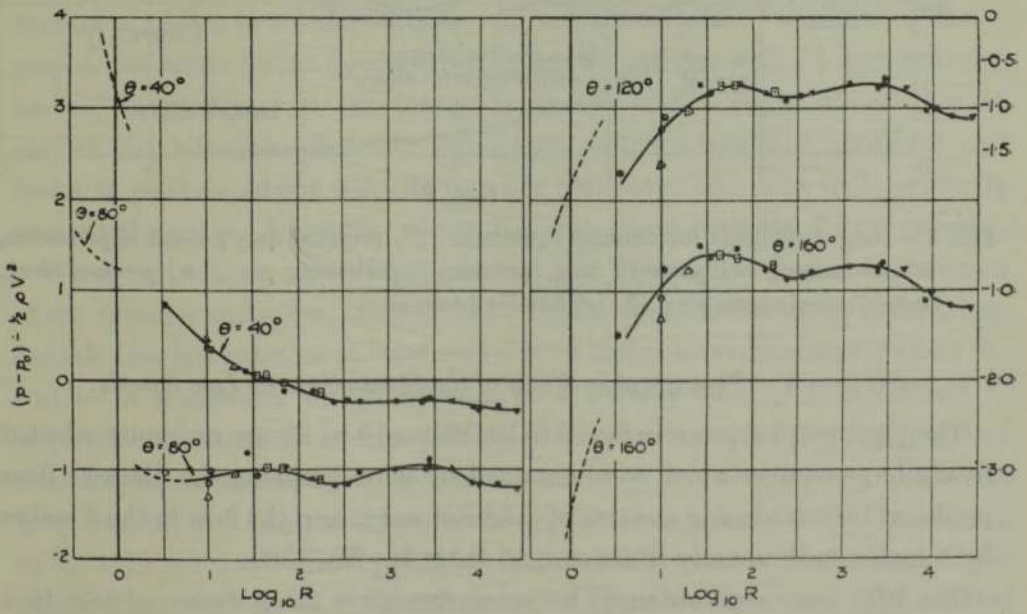

FIG. 7.—Pressure distribution round circular cylinders. △, theory ; ○, oil ; ⊡, water ; •, air ; ▲, air (Linke). Note :—Short dotted curves to right are plotted from Lamb's theory for very low Reynolds' numbers.

Fig. 7 shows the pressures, from the present experiments, from those of R. & M., No. 1194, and from the experiments of Linke. They are plotted for constant values of θ, namely, θ = 40°, 80°, 120° and 160°.

* 'Phys. Z.,' vol. 22, p. 321 (1921).

The points shown in triangles are from the arithmetical solutions, and the dotted lines show values obtained from Lamb's analytical solution.* Actually Lamb's solution only applies to values of R less than those shown, in fact to values much less than unity, but evidently in most cases the experimental results are converging with them.

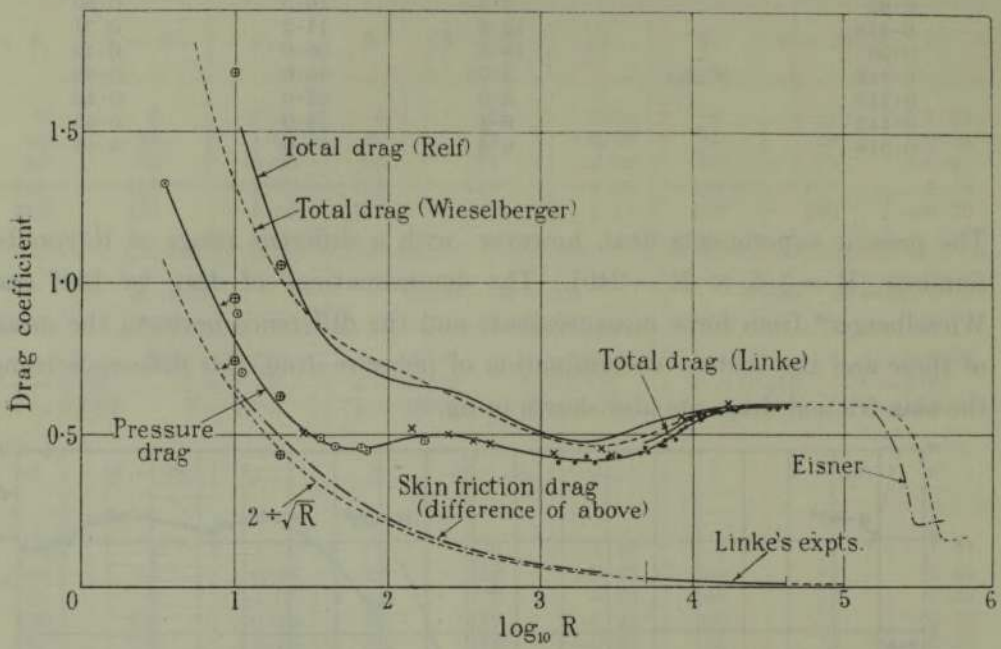

FIG. 8.—Drag coefficients for circular cylinders. ⊙, pressure drag present experiments, oil and water; ×, pressure drag, previous experiments, air; •, pressure drag, Linke's experiments, air; ⊕, arithmetical solutions.

Section 3.—*Photographic Study of the Streamlines at Low Speeds.*

The photographs shown in figs. 9 to 12, Plates 10 to 13, are examples selected from a large number which were obtained by photographing the filament lines produced by introducing streams of coloured water into the flow in the 5 inches by 5 inches tank already illustrated in R. & M., No. 1389.

The best lines were obtained by using fine glass tubes drawn almost to a point but uniform spacing is difficult to obtain in this manner. Accordingly a small brass tube was placed across the channel $2\frac{1}{2}$ inches from the bottom. On the *front* or upstream side of this tube were nine holes 1/64-inch diameter at 1/8-inch spacing from which the ink issued.

The study of the flow by filament lines is limited to low Reynolds' numbers, since it can only be used below the critical speed of the channel. Thus if R_c

* Lamb's 'Hydrodynamics,' 4 ed., pp. 581–583.

is the critical Reynolds' number for the channel, and d/l is the ratio of cylinder diameter to channel width, the method is only available up to $R = R_c\, d/l$. R_c was found to be about 2000. Hence if the maximum value of d/l is taken as 0·1, the limiting Reynolds' number for the cylinder is 200. This conclusion is quite independent of the size of channel used.

At very low speeds one of the difficulties met with is the tendency of the ink solution to sink. If the ink density is greater than that of water there is plenty of time for this to occur. For example the speed of the flow for fig. 11*a*, Plate 12, was 0·064 cm./sec. Convection currents are also troublesome.

A curious feature noticeable in figs. 10*a* and 11*a*, Plates 11 and 12, is the tendency of the nine streamlines to close up some distance behind the cylinder to a narrower width than they occupied in the undisturbed stream before they came to the cylinder. This is evidently a three dimensional effect produced by the interference of the walls and bottom. It can hardly indicate an increase in speed but rather a withdrawing of liquid from the plane of the streamlines.

The channel walls have evidently another effect, namely, to delay the production of eddies to a higher speed. An inspection of the two series of photographs, one taken with a $\frac{1}{4}$-inch cylinder, fig. 10, and one with a $\frac{1}{2}$-inch cylinder, fig. 11, shows this. In the former series the eddies begin about $R = 46$ and in the latter at $R = 62$. An $\frac{1}{8}$-inch cylinder was also examined and found to produce eddies when R was but little over 30. The walls evidently prevent the proper formation of the Kármán street with the $\frac{1}{2}$-inch cylinder.

When matters are adjusted so that an ink "streamline" strikes the front of the cylinder and splits, there is still a region close behind the cylinder where the ink does not enter, or at least only a trace enters by sinking slowly along the surface of separation and penetrating at a lower level. As it is difficult or impossible to arrange for such a splitting of a line to take place for any length of time a cylinder was fitted up so that ink could be extruded from a hole in the front generator. The photographs obtained with this arrangement are shown in fig. 12, Plate 13. The supply pipe for the ink is right at the bottom of the channel and the hole on the front generator $2\frac{1}{2}$ inches higher up. The gradual growth of the "kidney" eddy as the speed increases is clearly shown. That this region contains two closed eddies is shown by the difficulty of introducing ink into it and by the ink leaving the surface at right angles. This is further brought out in fig. 12*f* for which photograph the cylinder was turned through 180° so that the ink is emerging from the downstream generator. It travels forward to the "Ablösungspunkt" before it leaves the surface. This photograph has been taken at a higher value of R to show that this phenomenon

goes on when the periodic eddies are forming as well as at the lower speeds, showing that the stationary eddies, or at least kindred phenomena, are present along with the periodic eddies.

The frequency of the eddies (f) was obtained by counting the number formed per second. The values of the ratio fd/V so found when plotted on R shows nothing new, the points agreeing well with the values already found by oscillation experiments.†

The tendency for the ratio K/aV to fall with falling Reynolds' number is shown in Table III which contains particulars of the photographs in figs. 10 and 11. The strength of the eddies K must be zero for the Reynolds' number at which the periodic eddies cease to be formed. As already mentioned the periodic eddying behind the $\frac{1}{8}$-inch cylinder shows itself occasionally down to $R = 30$ but it is not very certain below about 36 unless the cylinder is released to oscillate with the appropriate period.

Table III.—Particulars of photographs shown in figs. 10 and 11, Plates 12 and 13.

Photograph.	Cylinder diameter d (cm.).	Velocity V (cm./sec.).	Eddy frequency f	Eddy separation a (cm.).	$R = Vd/\nu$.	fd/V.	K/aV.*
Fig. 10 *a*	0·635	0·067	—	—	3·8	—	—
Fig. 10 *b*	0·635	0·21	—	—	11·0	—	—
Fig. 10 *c*	0·635	0·82	—	—	43·0	—	—
Fig. 10 *d*	0·635	0·93	0·20	4·3	49·0	0·14	0·22
Fig. 10 *e*	0·635	1·02	0·21	4·35	54·0	0·13	0·29
Fig. 10 *f*	0·635	1·97	0·41	3·8	103·0	0·13	0·59
Fig. 11 *a*	1·27	0·064	—	—	7·2	—	—
Fig. 11 *b*	1·27	0·22	—	—	23·0	—	—
Fig. 11 *c*	1·27	0·474	—	—	50·0	—	—
Fig. 11 *d*	1·27	0·634	0·077	—	71·0	0·15	—
Fig. 11 *e*	1·27	0·85	0·11	—	88·0	0·17	—
Fig. 11 *f*	1·27	2·0	0·27	—	208·0	0·17	—

* $K/aV = (1 - af/V)\sqrt{8}$.

In the previous experiments on oscillating cylinders only very small cylinders were used for the lowest values of R. Repeat experiments using the $\frac{1}{8}$-inch diameter cylinder gave the same results, namely, at $R = 33$ oscillation would take place if the natural frequency was adjusted to give fd/V anything between

† R. & M., No. 1373, fig. 7, or 'Phil. Mag.,' fig. 3, vol. 12, p. 493 (1931).

0·097 and 0·15, and at R = 28 no oscillation could be obtained at any period. From R = 29 to about R = 35 it seems better to say that the oscillation causes the eddying rather than the eddying the oscillation.

The author previously assumed* that the eddies produced a circulation which produced the side force necessary to maintain the oscillation. An examination through a low power microscope of the ink filament lines in front of the fixed cylinder while eddies were being given off, showed no periodic wavering such as would be expected with a periodic circulation.† It follows either that the eddies produce no circulation or that the circulation is only present when the cylinder is oscillating.

There would seem to be a possible alternative explanation of the phenomenon of oscillation other than that it is produced entirely by the periodic eddies.

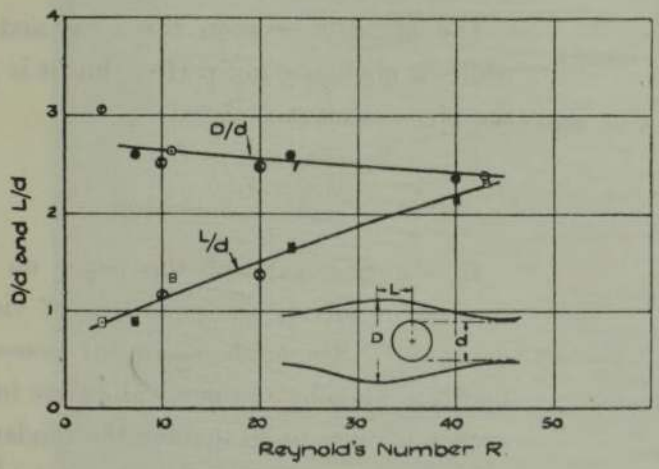

FIG. 13.

Is it not possible that the kidney eddies play a part in the following manner? These are, as it were, attached to the cylinder and hence when it is oscillating and approaches the end of its swing they continue, in the same direction long enough to set up a circulation by dragging the liquid round the cylinder with them. The circulation so produced would be of the correct sign to apply the force to drive the cylinder back towards the centre.

To test this hypothesis an $\frac{1}{8}$-inch diameter cylinder was fitted with a vane along its entire length, fig. 14. This vane was free to rotate about the cylinder

* R. & M., No. 1373, *loc. cit.*

† Other experimenters claim to have observed this wavering, but probably the Reynolds' number was different.

axis being carried on two needles. The arrangement* was found to oscillate at channel speeds above 2·2 cm./sec. (R = 58). For each water speed there was a band of frequencies which gave the maximum amplitude generally corresponding roughly to $fd/V = 0{\cdot}03$ to $0{\cdot}06$. The most interesting point is, however, that the oscillation is very much more vigorous if the cylinder is inclined so that the top is further upstream than the bottom. This was discovered by accident although it might have been expected in view of the explanation given above. Towards the end of the swing the weight of the vane (once it has passed a certain position) is rotating it in the direction necessary for the required circulation. Obviously, however, with the inclined cylinder low water speeds are impossible as the vane falls right over on one side or the other.

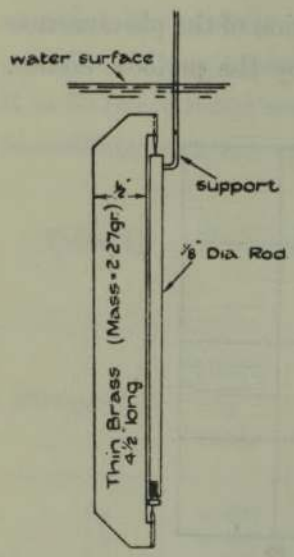

FIG. 14.

The analogy between the vane and the kidney eddies is obviously not perfect, but it is possible that the phenomena are related.

Summary.

In the first part of the paper an arithmetical method of solving the equations of viscous flow is developed. The method is one of successive approximations, whereby the new values are interpolated in such a manner as to involve the fundamental equations being solved. A development of the method involves the use of an auxiliary solution to obtain first a conformal network for the given boundaries. The solution is then carried out on this network. This procedure avoids certain boundary difficulties.

The method is applied to obtain the flow past a circular cylinder at Reynolds' number 20. Two weak symmetrical eddies are obtained behind the cylinder. Values for the drag and pressure distribution are also given.

In the second part of the paper measurements of the pressure round cylinders at very low Reynolds' numbers are given. These are shown to agree with the theoretical values of the first part. A comparison with the measured total drag obtained by other experimenters enables the skin friction drag to be determined.

* The whole unit was free to oscillate across the channel, as in the experiments described in R. & M. No. 1373, *loc. cit.*

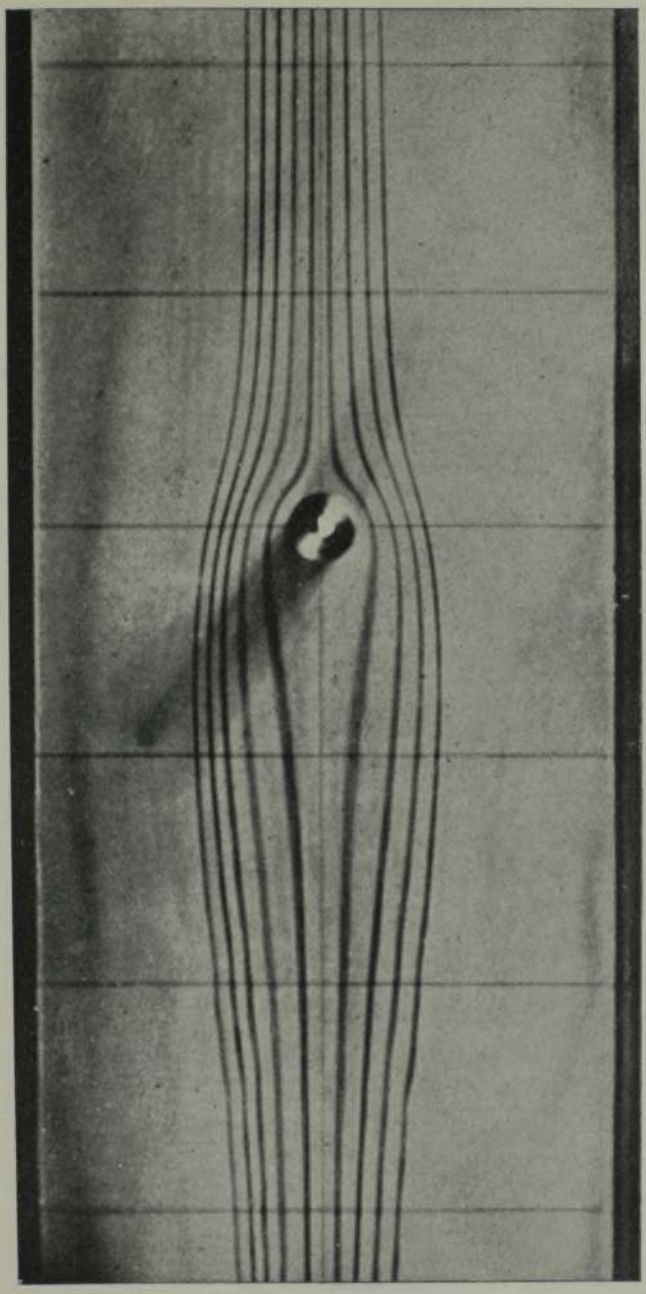

FIG. 9.—$\frac{1}{2}$-in. cylinder in a 5-in. channel. $R = Vd/\nu = 23$.

(*Facing p.* 668.)

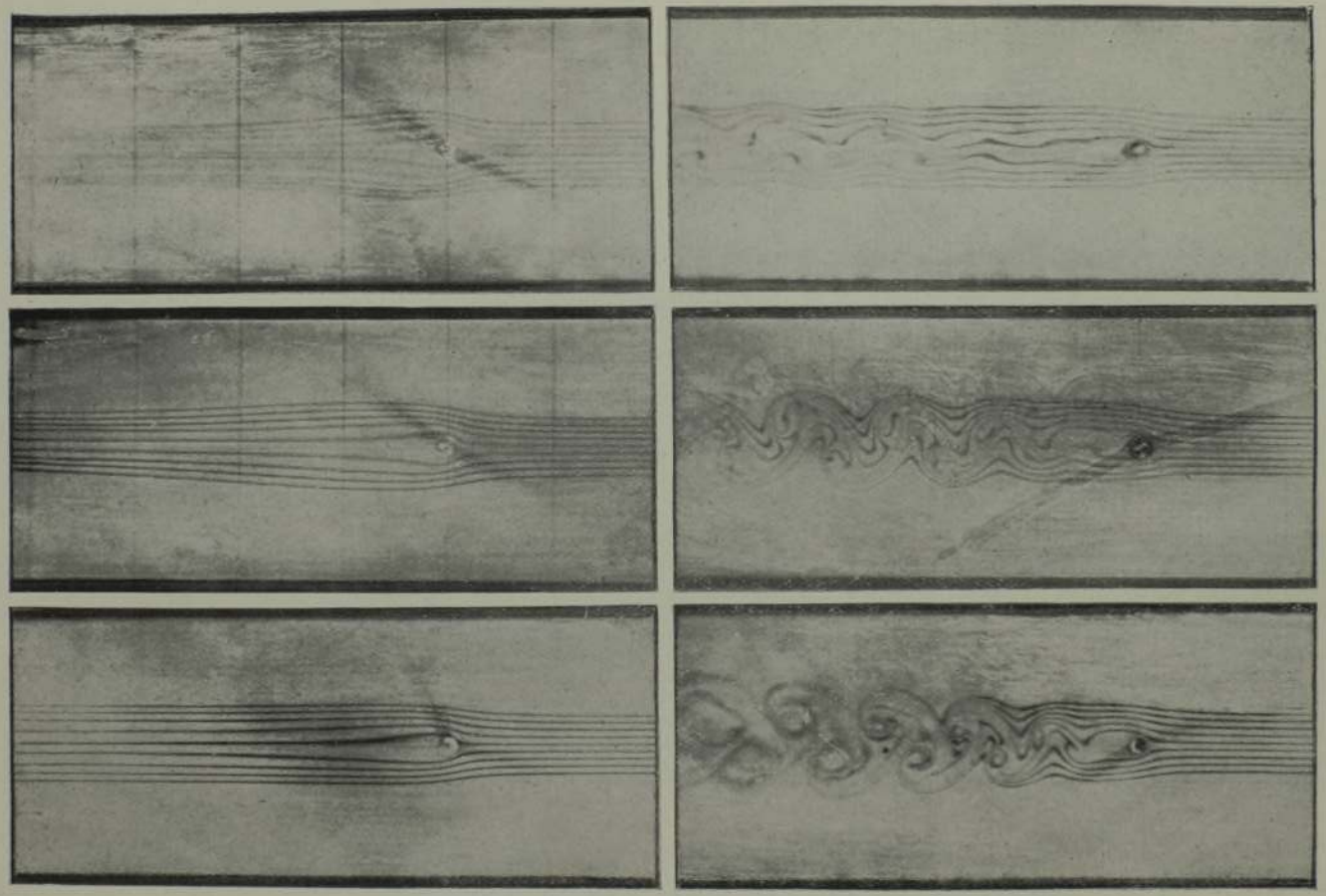

FIG. 10.—$\frac{1}{4}$-in. cylinder in a 5-in. channel.

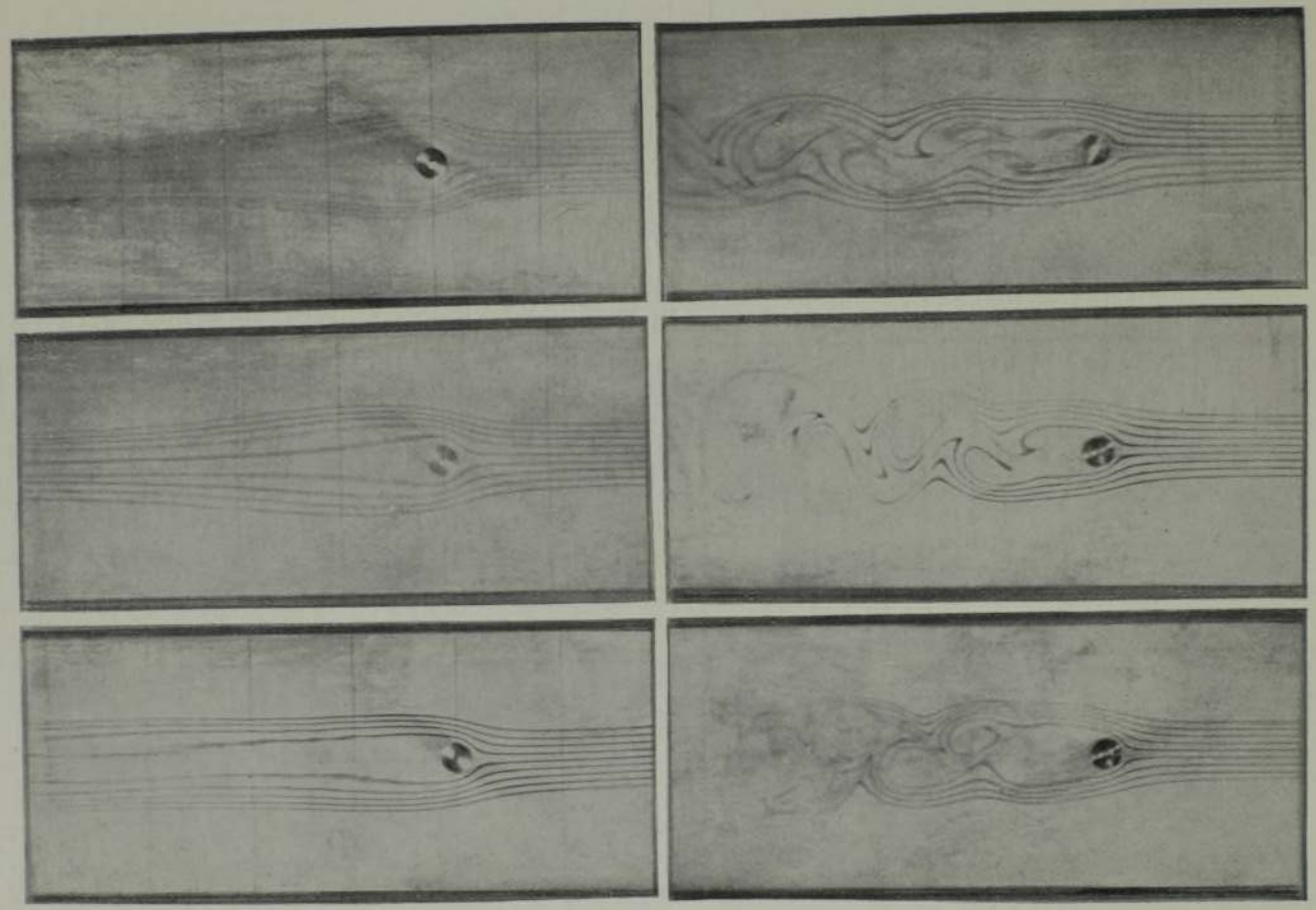

FIG. 11.—½-in. cylinder in a 5-in. channel.

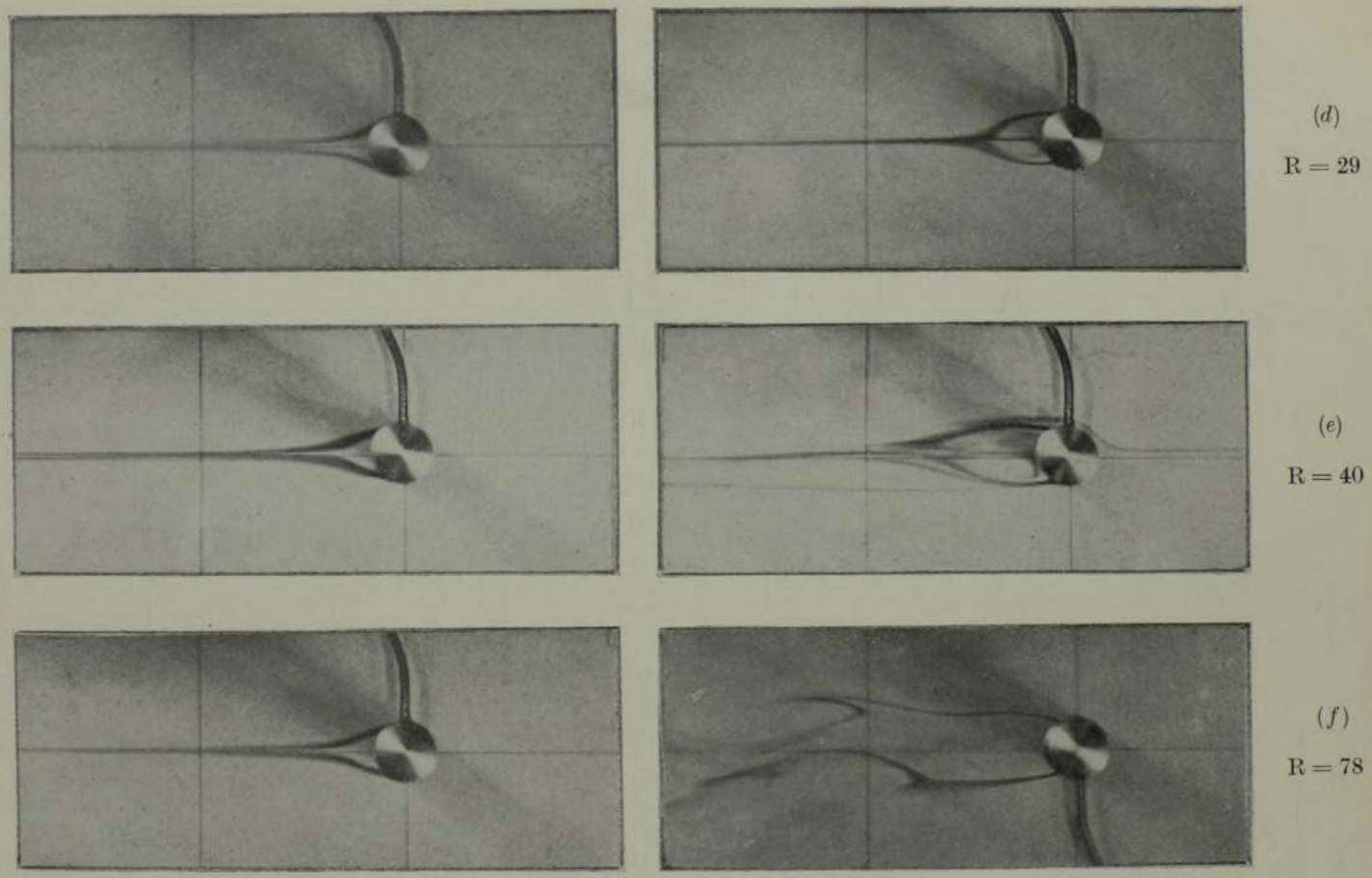

FIG. 12.—$\frac{1}{2}$ diameter cylinder.

In the last part a set of photographs of the streamlines past a cylinder is given. A comparison of the theoretical solution with these shows a good agreement. The photographs also show the gradual development and growth of the symmetrical stationary eddies behind the cylinder as the speed increases, followed by the development of the Kármán street. The exact Reynolds' number at which the latter first develops is shown to be affected by the presence of the channel walls.

On the Ionization of Light Gases by X-Rays. I.—*Technique.*

By W. R. Harper, Wills Physics Laboratory, University of Bristol.

(Communicated by Lord Rutherford, O.M., F.R.S.—Received April 26, 1933.)

Introduction.

The measurement of the intensity of an X-ray beam in absolute units is in theory most satisfactorily accomplished by a determination of its heating effect. The method, however, is attended by considerable experimental difficulties, so that its application is very limited, and in practice it is usual to replace it by a determination of the ionization produced when the beam is passed through a gas. To correlate the ionization with an absolute intensity requires a quantitative knowledge of the details of the interaction between the X-rays and the molecules concerned and of the ionization of the gas by the ejected electrons. It sometimes happens that the processes involved about which we know least are relatively unimportant, so that a fairly reliable correlation can be made; and much work has been done on the application of the ionization method to X-ray dosimetry. But in general a quantitative correlation between ionization and intensity is not possible. A further study of the ionization of gases by X-rays is therefore desirable; moreover it may be made to yield important information concerning the processes involved. The early development of the physics of X-rays contains many examples of this, and more recently an important contribution has been made by Stockmeyer.*

The events leading to the ionization of a heavy gas are exceedingly complicated, whereas in the light gases (hydrogen and helium) some of these events

* 'Ann. Physik,' vol. 12, p. 71 (1932).